



Short communication

Discovery of novel non-covalent inhibitors selective to the $\beta 5$ -subunit of the human 20S proteasomeKai Xu ^a, Ke Wang ^a, Ying Yang ^a, Ding-An Yan ^a, Li Huang ^b, Chin-Ho Chen ^b, Zhiyan Xiao ^{a,*}^a Beijing Key Laboratory of Active Substance Discovery and Druggability Evaluation, Institute of Materia Medica, Chinese Academy of Medical Sciences and Peking Union Medical College, Beijing 100050, China^b Department of Surgery, Duke University Medical Center, Durham, NC 27710, USA

ARTICLE INFO

Article history:

Received 14 August 2014

Received in revised form

14 May 2015

Accepted 14 May 2015

Available online 16 May 2015

Keywords:

Proteasome inhibitors

Non-covalent

Linear peptides

Selectivity

Fragment-based approach

ABSTRACT

A series of linear peptides (**6a–6o**) were designed based on the known non-covalent 20S proteasome inhibitors TMC-95A and compound **5** via a fragment-based approach. These compounds were synthesized and evaluated against the chymotrypsin-like activity of the human 20S proteasome. Three of them (**6d**, **6e** and **6k**) were potent inhibitors with IC₅₀ values at the submicromolar level. These three compounds were selective to the $\beta 5$ -subunit and showed no obvious inhibition against trypsin-like and caspase-like activities of the human 20S proteasome. Docking study of the most potent compound **6e** revealed its key interactions with the $\beta 5$ -subunit of the 20S proteasome. These findings have provided a new chemical template for non-covalent proteasome inhibitors, which is ready for further structural optimization to improve both potency and subunit selectivity.

© 2015 Elsevier Masson SAS. All rights reserved.

1. Introduction

The ubiquitin-proteasome system (UPS) is a proteolytic pathway precisely regulating the cellular protein homeostasis via enzymatic cascades [1]. The 20S proteasome is the main proteolytic component of the UPS. In eukaryotes, the $\beta 5$, $\beta 2$ and $\beta 1$ subunits of the 20S proteasome are responsible for chymotrypsin-like, trypsin-like, and caspase-like proteolytic activities, respectively [2]. The 20S proteasome has been regarded as a potential therapeutic target for the treatment of various pathological conditions. The successful development of 20S proteasome inhibitors, bortezomib [3] and carfilzomib [4], into anti-cancer drugs has made the 20S proteasome a validated target for cancer chemotherapy. However, both bortezomib and carfilzomib are covalent proteasome inhibitors and are associated with the problems of severe side effects, acquired drug resistance, and unsatisfactory pharmacokinetic profiles. Therefore, it is imperative to search for novel non-covalent proteasome inhibitors as potential chemotherapeutic agents. Up to now, peptide-based proteasome inhibitors remain to be the

mainstream in this field [5], although peptidomimetic [6], pseudopeptide-based [7] and non-peptidic [8–10] inhibitors have been recently reported.

TMC-95A (Fig. 1a) is a natural cyclic tripeptide isolated from fermentation broth of the ascomycete fungus *Apiospora montagnei* [11]. It is a very potent inhibitor of the 20S proteasome and inhibits the chymotrypsin-like (ChT-L) activity of the 20S proteasome with an IC₅₀ value of 5.4 nM [11,12]. In contrast to bortezomib and carfilzomib, TMC-95A is a non-covalent inhibitor of the 20S proteasome [13], which may have a better pharmacological profile with reduced side effects. In spite of its high potency and unique interaction mode, its structural complexity impedes the development of efficient total synthesis. Instead, TMC-95A has become a prototype molecule for the discovery of novel non-covalent proteasome inhibitors.

The crystal structure of 20S proteasome: TMC-95A complex reveals the binding mode of TMC-95A in the active sites of the 20S proteasome [13]. Besides hydrogen bonds formed with the peptide backbone, TMC-95A interacts with the 20S proteasome mainly by the (Z)-prop-1-enyl group and the asparagine residue, which protrude into the S1 and S3 pockets of the active sites, respectively (Fig. 1b). In contrast, only weak interaction between the tyrosine residue and the shallow hydrophobic S4 pockets is observed, and

* Corresponding author.

E-mail address: xiaoz@imm.ac.cn (Z. Xiao).

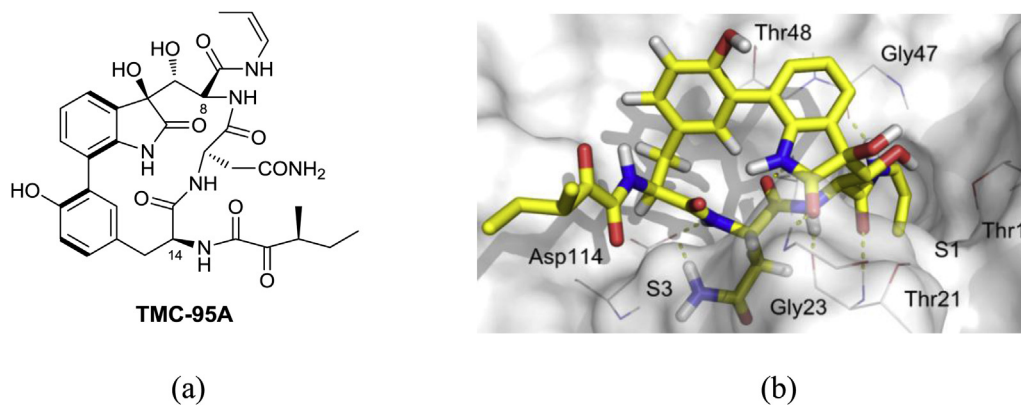


Fig. 1. The structure of TMC-95A (a) and its interaction mode with the β_2 subunit of 20S proteasome (b).

the 3-methyl-2-oxopentanoyl group seems to contribute little to the binding affinity [13]. Such interaction modes have manifested the importance of the moieties interacting with S1 and S3 pockets and insights from the crystallographic analysis have eventually led to the discovery of several synthetically less challenging analogs of TMC-95A (Fig. 2). Danishefsky et al. synthesized a series of simplified TMC-95A analogs by replacing the *cis*-propylene residue on the C8 side chain of TMC-95A with more readily available groups, and eliminating the chiral center on the C14 side chain. Most of the analogs (e.g. compound **1**) retained inhibitory potency against the 20S proteasome [14]. Further simplification of the functionalities on the TMC-95A core resulted in the identification of compound **2** and its analogs. Crystallographic study on complex structures between the 20S proteasome and these analogs revealed a binding mode similar to that of TMC-95A [15]. To simplify the core skeleton of TMC-95A, endocyclic biphenyl-ether derivatives were synthesized, which had the complex biaryl moiety in TMC-95A substituted with a biphenyl ether. Such structural alteration

resulted in the preservation of key interactions with the active site so as to retain the proteasome inhibition. Compound **3** is a representative structure of this compound series [16,17]. Various linear analogs of TMC-95A were also synthesized to further simplify the core skeleton of TMC-95A [18,19]. As illustrated by the structure of compound **4**, the tripeptide backbone of TMC-95A was maintained, however, the cyclic core scaffold was dissected at the covalent bond between the two aryl groups. Compound **4** retained the key interactions with the active sites of the 20S proteasome, though due to the loss of rigidity, it assumed a more extending conformation in the active site [19]. Notably, the linear construct seemed to provide a versatile skeleton for structural optimization to modulate inhibitory potency toward different β subunits [18].

Other linear peptides have also been previously reported as potent proteasome inhibitors and interestingly, most of them showed apparent selectivity to the β_5 -subunit of the 20S proteasome, which is believed to be a potential advantage over simultaneous inhibition of all the three subunits [20]. 5-Methoxy-1-

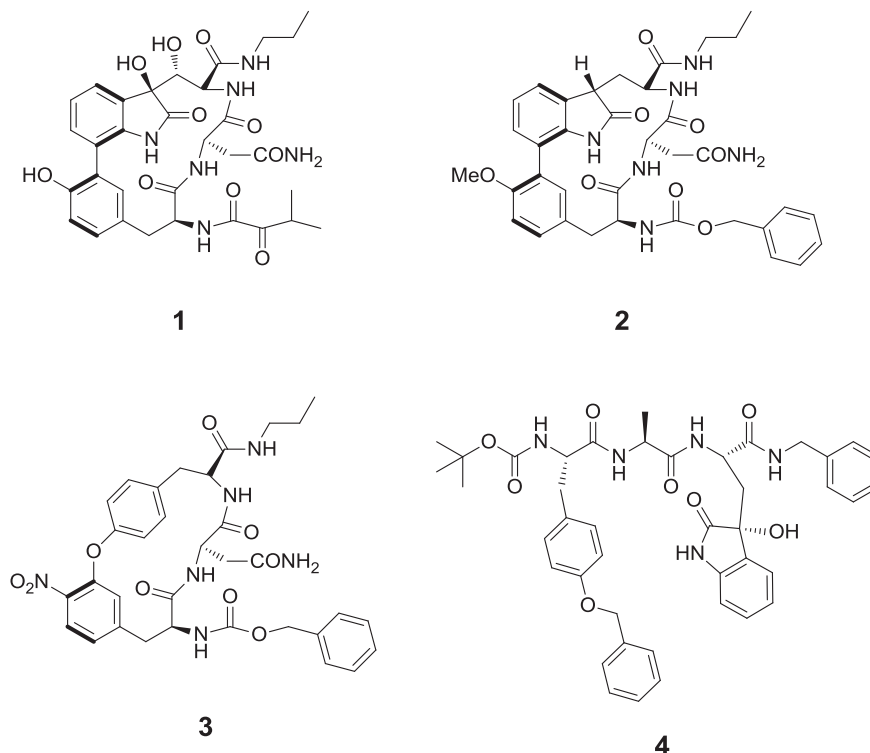


Fig. 2. Representative simplified TMC-95A analogs.

indanone capped di- and tripeptides were the first structural class reported as selective inhibitors for the ChT-L activity of the 20S proteasome [21,22]. In addition, a novel series of capped di- and tripeptides originated from high-throughput screening were also identified as non-covalent proteasome inhibitors with selectivity toward the $\beta 5$ -subunit [23,24]. A series of 2-aminobenzylstatine derivatives, which were originally designed to target the HIV-1 proteinase, were found to be non-covalent inhibitors specifically inhibiting the ChT-L activity of the 20S proteasome [25]. Molecular docking [26] and subsequent structure-based optimization [27,28] led to the discovery of compound **5**, which is a dipeptide-based proteasome inhibitor selective to the $\beta 5$ -subunit and active in cellular assays [28]. Molecular modeling study [28] reveals the interaction mode between the $\beta 5$ subunit of the 20S proteasome and compound **5** (Fig. 3), which underscores the hydrophobic interactions between the AS1 and AS2 pockets of the active site and the 3-phenoxyphenylacetyl moiety in compound **5** (Fig. 3). The structure of compound **5** provides a new chemical template for further design of non-covalent proteasome inhibitors selective to the $\beta 5$ -subunit of the 20S proteasome.

2. Molecular design

Based on the chemical templates of both TMC-95A and compound **5**, we report herein the discovery of a novel series of non-covalent proteasome inhibitors via a fragment-based drug design approach. Compound **6a** (Fig. 4 and Table 1) was first designed by incorporating the S1/S3 fragments in TMC-95A analogs and the AS1/AS2 fragments in compound **5**. As expected, compound **6a** exhibited significant inhibition against the ChT-L activity of the 20S proteasome with an IC_{50} of 12.97 μM . This result encouraged us to further modify the P1 and P3 areas of compound **6a** to improve its potency. A series of compounds with the general formula of **6** were thereby designed and synthesized. Compound **6b** and **6c** introduced a hydroxyl group in R^2 to examine the possibility of forming additional hydrogen bonds with the active sites. Compounds **6d–6f** further furnished the n -propyl group in **6a** with various substituents. Compounds **6g–6l** were designed following the fragment-based strategy by incorporating at R^2 various “S1 fragments” from previously reported non-covalent proteasome inhibitors to explore SAR in this molecular area [24,28]. Compounds **6m–6o** were intended to check the effects of the S3 moiety on proteasome inhibitory activity by altering the asparagine residue in R^1 .

3. Chemistry

The synthesis of the desired compounds is shown in Scheme 1. The corresponding Boc protected amino acids and H-L-Val-OBn were coupled in the presence of 2-(1H-7-azabenzotriazol-1-yl)-

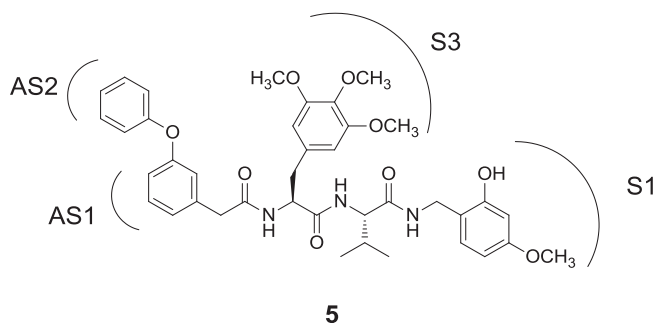


Fig. 3. Schematic representation of the interaction mode between compound **5** and the $\beta 5$ -subunit of the 20S proteasome.

1,1,3,3-tetramethyl-uronium hexafluorophosphate (HATU) and N,N -diisopropylethylamine (DIEA) to give a dipeptide scaffold. The dipeptide was then treated with trifluoroacetic acid to free the amino group, which was further coupled with 3-phenoxyphenylacetic acid to give compound **6g**. **6g** was subjected to hydrogenation in the presence of 10% Pd/C to yield compound **6c**. **6c** was subsequently coupled with the corresponding amines to afford **6a**, **6b**, **6d**, **6e** and **6h–6n**. **6f** and **6o** were obtained by hydrogenation of **6d** and **6n**, respectively.

4. Results and discussion

All synthesized compounds were assayed for their inhibitory potency against the ChT-L activity of the human 20S proteasome as described previously [29], and lactacystin was used as a reference compound. As shown in Table 1, most compounds showed significant inhibitory potency against the ChT-L activity of the human 20S proteasome. Among them, **6d**, **6e**, **6k** and **6m** exhibited IC_{50} values at lower micromolar or even submicromolar levels. These results suggested that our molecular design strategy is effective in identifying novel linear peptides as potent proteasome inhibitors.

Preliminary SAR could be deduced from the data listed in Table 1. When the terminal methyl in R^2 of compound **6a** was replaced with a hydroxyl, the inhibition potency was slightly decreased (**6a** vs **6b**). While truncation of the side chain at R^2 could result in dramatic loss of potency (**6b** vs **6c**). Incorporation of additional substituents on the n -propyl group of **6a** could lead to significant improvement in potency (**6a** vs **6d/6e**), however, appropriate steric or electronic properties of the substituents might be required (**6e** vs **6f**). Variation at R^2 could cause substantial difference in inhibitory potency, presumably due to the different affinity to the S1 pocket (**6g–6l**). Among the “S1 fragments” investigated, the (2-hydroxy-4-methoxybenzyl)amino group (cf. compound **6k**) was identified as the optimal S1 moiety for further SAR exploration on R^2 . Extension of the R^1 side chain in compound **6k** by one carbon (compound **6m**) could slightly decrease the potency. Replacing the R^1 side chain with a basic residue (compound **6o**) could lead to significant loss of inhibitory potency. However, extending the terminal amino with benzyloxycarbonyl (compound **6n**) could partially restore the potency.

Three compounds **6d**, **6e** and **6k** with the most potent inhibitory activity against ChT-L activity were further evaluated against $\beta 1$ - and $\beta 2$ -subunits. The compounds were tested in a series of four-fold dilutions (10, 2.5, 0.625, 0.156 and 0.039 $\mu g/mL$) and none of them showed percentage inhibition above 50% against trypsin-like and caspase-like activities even at the highest tested concentration. The results suggested that this novel series of proteasome inhibitors could be selective to the $\beta 5$ -subunit of the 20S proteasome, which is consistent with the previous observations on linear peptide proteasome inhibitors.

A docking study on the most potent compound **6e** indicated that the compound could occupy the active site between $\beta 5$ and $\beta 6$ subunits of the 20S proteasome. The 2D- and 3D-plots of key interactions between compound **6e** and the 20S proteasome were illustrated in Fig. 5. As expected, the tripeptide backbone formed several hydrogen bonds with the active site residues (e.g. Thr 21, Gly 47 and Ala 49 in the $\beta 5$ subunit and Asp 114 in the $\beta 6$ subunit). The R^1 and R^2 side chains of compound **6e** extended to the S3 and S1 pockets of the active site, respectively. Hydrogen bonds were also observed between the hydroxyl group in R^2 and Thr1 of the $\beta 5$ subunit, as well as the carbonyl oxygen atom in R^2 and Gly 47. This could at least partly explain a more than 40-fold increase in potency of **6e** as compared with compound **6a**. Furthermore, π - π stacking and π -cation interactions were also detected between residues Tyr 96, His 98 and the phenoxyphenyl moiety, which is in consistence

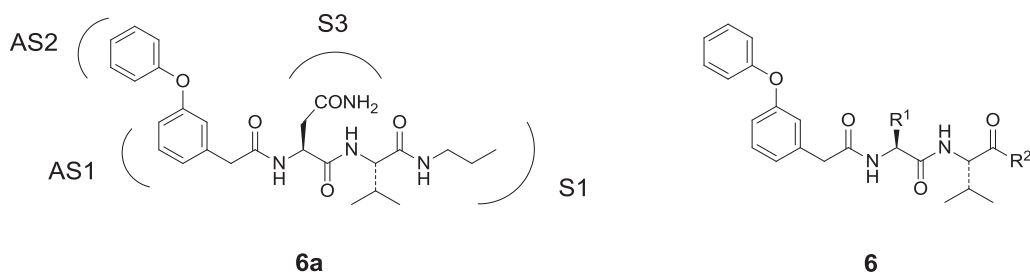
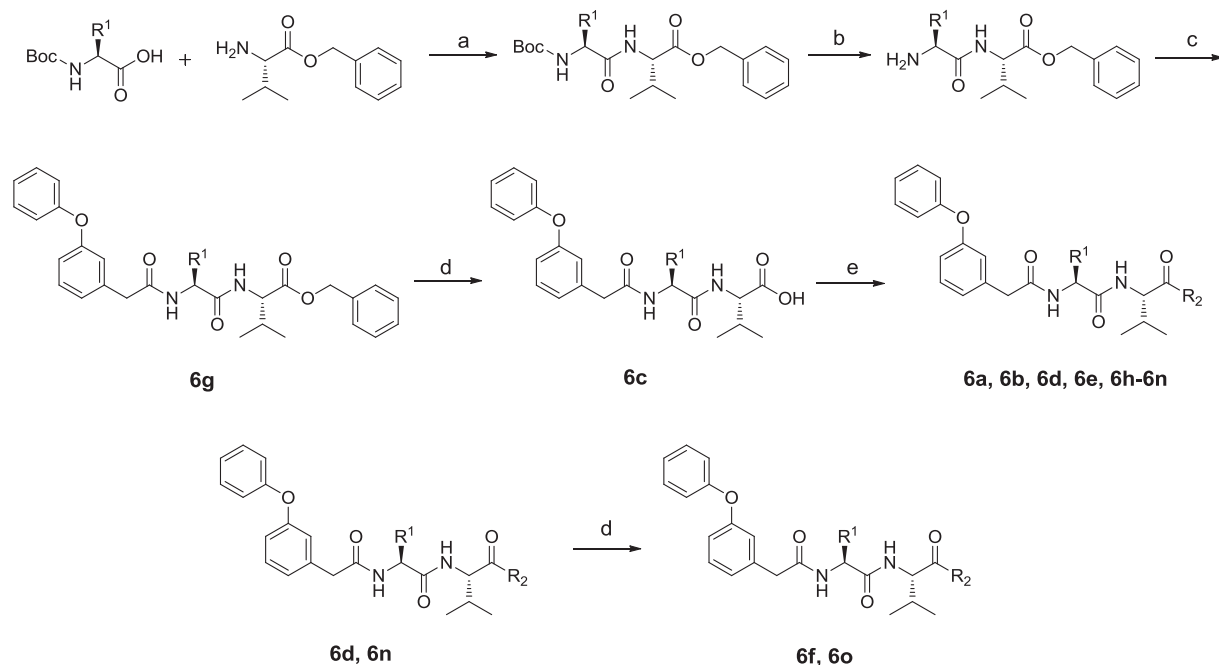


Fig. 4. Molecular design of the target compounds.



Scheme 1. Synthesis of compound **6a-6o**.^a Reagents and conditions: (a) HATU, DIEA, DMF, r.t., overnight; (b) CF_3COOH , DCM, r.t., 4 h; (c) 3-phenoxyphenylacetic acid, HATU, DIEA, DMF, r.t., overnight; (d) 10% Pd/C, MeOH, H_2 , overnight; (e) appropriate amines, HATU, DIEA, DMF, r.t., overnight. ^a R^1 , R^2 are defined in Table 1.

with the molecular design to implant this “fragment” so as to induce additional interactions with the accessory subpockets of the 20S proteasome.

5. Conclusion

A series of linear peptides were designed based on the chemical templates of TMC-95A and compound **5** via a fragment-based design strategy. The *N*-terminal of the peptides was extended with the 3-phenoxyphenylacetyl moiety to form additional interactions with accessory subpockets in the active sites. For most compounds, the asparagine residue in TMC-95A was preserved as the “S3 fragment”, while the (*Z*)-prop-1-enyl group was modified or replaced with various more readily available “S1 fragments” from known proteasome inhibitors. New linear peptides with IC_{50} values at submicromolar concentrations against the ChT-L activity of the human 20S proteasome have been identified. Notably, these compounds exhibited significant selectivity toward the $\beta 5$ -subunit of the human 20S proteasome. Docking study on the most active compound **6e** revealed key interactions between **6e** and the $\beta 5$ -subunit of the 20S proteasome. These novel linear peptide proteasome inhibitors provides a versatile chemical template ready for further structural optimization to modulate potency and selectivity.

6. Experimental section

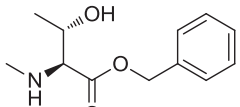
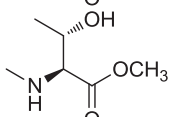
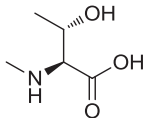
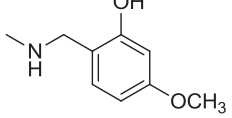
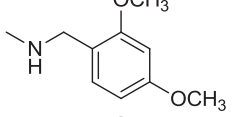
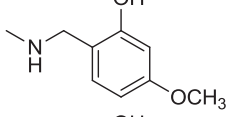
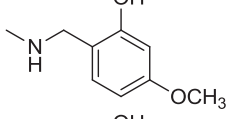
6.1. Material and measurements

All reactions were monitored by thin-layer chromatography with pre-coated silica gel F254 plates purchased from Merck, Inc. All melting points were determined on Yanaco Melting point apparatus and were uncorrected. Mass spectra (MS) were taken in ESI mode on Agilent Technologies LC/MSD TOF instruments. ^1H NMR spectra were recorded on Varian Mercury 300-MHz or 400-MHz spectrometer. ^{13}C NMR spectra were recorded on Bruker AV-III-500 spectrometer. Chemicals were obtained from local suppliers and were used without further purification.

6.2. Preparation and characterization of compounds **6a-6o**

A 125 ml round bottom flask was charged with a magnetic stir bar, Boc-Asn-OH (3.032 g, 13 mmol), H-L-Val-OBzl·TosOH (4.955 g, 13 mmol), HATU (4.965 g, 13 mmol), DIEA (4.200 g, 32.5 mmol) and DMF (40 ml) were then added. The mixture was stirred under ice bath for 1 h and then stirred overnight at room temperature. After removal of the solvent under reduced pressure, the residue was dissolved in ethyl acetate and sequentially washed by 1 M

Table 1
Inhibition against the ChT-L activity of the human 20S proteasome by compounds **6a–6o**.

Compd	R ¹	R ²	IC ₅₀ (μM) ^a
6a	CH ₂ C(O)NH ₂	NH(CH ₂) ₂ CH ₃	12.97 ^b
6b	CH ₂ C(O)NH ₂	NH(CH ₂) ₂ OH	17.19 ^b
6c	CH ₂ C(O)NH ₂	OH	NA ^d
6d	CH ₂ C(O)NH ₂		0.92 ^c
6e	CH ₂ C(O)NH ₂		0.29 ^c
6f	CH ₂ C(O)NH ₂		13.88 ^b
6g	CH ₂ C(O)NH ₂	OBz	17.31 ^b
6h	CH ₂ C(O)NH ₂	NH(CH ₂) ₂ Ph	NA
6i	CH ₂ C(O)NH ₂	(<i>R</i>)-NHCH(CH ₃)Ph	NA
6j	CH ₂ C(O)NH ₂	(<i>S</i>)-NHCH(CH ₃)Ph	NA
6k	CH ₂ C(O)NH ₂	OH	0.66 ^c
6l	CH ₂ C(O)NH ₂		NA
6m	(CH ₂) ₂ C(O)NH ₂		1.63 ^b
6n	(CH ₂) ₄ NHCbz		11.73 ^b
6o	(CH ₂) ₄ NH ₂		NA
Lactacystin			10.09 ^c

^a The IC₅₀ values are for inhibition against the ChT-L activity of the human 20S proteasome.

^b The IC₅₀ values are the averages from two independent experiments.

^c The IC₅₀ values are the averages from three independent experiments.

^d NA, not active. No significant inhibition was observed at a series of four-fold dilutions (10, 2.5, 0.625, 0.156 and 0.039 μg/mL).

hydrochloride acid, saturated sodium bicarbonate and brine. The organic layer was dried over anhydrous sodium sulfate. 5.2 g white solid was obtained after removal of the solvent. 3.006 g white solid was dissolved in TFA/DCM (18 ml/20 ml), the mixture was stirred overnight at room temperature. Then the solvent was removed under reduced pressure to give a light yellow oil which is used for the next step without further purification. DMF (40 ml), 3-phenoxyphenylacetic acid (1.628 g, 7.13 mmol), HATU (2.715 g, 7.13 mmol) and DIEA (9.228 g, 7.13 mmol) were sequentially added to the oil obtained. The mixture was stirred overnight at room temperature then the solvent was removed under reduced pressure. The residue was dissolved in ethyl acetate and sequentially

washed by 1 M hydrochloride acid, saturated sodium bicarbonate and brine. The organic layer was dried over anhydrous sodium sulfate. After concentrated, 1.366 g **6g** (yield: 36.0% for steps a–c in Scheme 1) was afforded by column chromatography (DCM:MeOH = 80:1). **6g** (1.366 g) was suspended in methanol (100 ml) with 10% Pd/C (130 mg), and stirred overnight at room temperature under hydrogen atmosphere. After filtration, the filtrate was concentrated to give 1.040 g **6c** (yield: 91.7%). **6c** (0.220 g, 0.5 mmol), *n*-propylamine (0.030 g, 0.5 mmol), HATU (0.190 g, 0.5 mmol) and DIEA (0.162 g, 1.25 mmol) were dissolved in DMF (15 ml), the mixture was then stirred overnight at room temperature. The reaction mixture was concentrated and the resulting residue was purified by column chromatography (DCM:MeOH = 20:1) to give the desired compound **6a** (54 mg, yield: 22.5%).

Compounds **6b**, **6d**, **6e** and **6h–6n** were synthesized with the experimental protocols described for compound **6a**.

Compound **6d** (0.632 g, 1 mmol) was dissolved in methanol and 10% Pd/C (0.060 g) was added to the solution. The reaction mixture was stirred at room temperature overnight. After filtration, the filtrate was concentrated to give 0.541 g **6f** (yield: 99.0%).

Compound **6o** was synthesized from **6n** with the protocols described for **6f**.

6.2.1. *N*-2-(3-phenoxyphenyl)acetyl-*L*-Asn-*L*-Val-NH(CH₂)₂CH₃ (**6a**)

Yield: 22.5%; mp: 236.0–238.0 °C; ¹H NMR (CD₃OD, 300 Hz): δ 7.29–7.17 (m, 3H), 7.05–6.96 (m, 2H), 6.92–6.89 (m, 3H), 6.79–6.75 (dd, 1H, *J* = 1.5, 8.4 Hz), 4.71–4.66 (t, 1H, *J* = 6.6 Hz), 4.06–4.04 (d, 1H, *J* = 6.0 Hz), 3.46 (s, 2H), 3.08–3.02 (m, 2H), 2.74–2.66 (m, 1H), 2.57–2.50 (m, 1H), 2.08–1.99 (m, 1H), 1.50–1.38 (m, 2H), 0.85–0.76 (m, 9H); ¹³C NMR (DMSO-*d*₆, 125 Hz): δ 172.1, 171.3, 170.8, 170.3, 157.1, 156.9, 138.8, 130.5, 130.1, 124.7, 123.8, 119.9, 119.0, 117.0, 58.1, 50.1, 42.2, 40.7, 37.3, 30.7, 22.7, 19.6, 17.9, 11.9; MS-ESI *m/z*: 483 [M+H]⁺.

6.2.2. *N*-2-(3-phenoxyphenyl)acetyl-*L*-Asn-*L*-Val-NH(CH₂)₂OH (**6b**)

Yield: 22.8%; mp: 162.0–166.0 °C; ¹H NMR (CD₃OD, 300 Hz): δ 7.27 (t, 2H, *J* = 5.7 Hz), 7.21 (t, 1H, *J* = 6.0 Hz), 7.05–6.97 (m, 2H), 6.92–6.90 (m, 3H), 6.78 (d, 1H, *J* = 6.0 Hz), 4.70 (t, 1H, *J* = 5.1 Hz), 4.10 (d, 1H, *J* = 4.2 Hz), 3.52 (t, 2H, *J* = 4.5 Hz), 3.47 (s, 2H), 3.28–3.19 (m, 2H), 2.76–2.70 (m, 1H), 2.58–2.52 (m, 1H), 2.13–2.05 (m, 1H), 0.79 (t, 6H, *J* = 4.5 Hz); ¹³C NMR (DMSO-*d*₆, 150 Hz): δ 172.2, 171.2, 171.1, 170.3, 157.1, 156.9, 138.7, 130.5, 130.1, 124.7, 123.8, 119.9, 119.0, 117.0, 60.2, 58.0, 50.1, 42.2, 41.9, 37.2, 30.7, 19.6, 17.9; MS-ESI *m/z*: 485 [M+H]⁺.

6.2.3. *N*-2-(3-phenoxyphenyl)acetyl-*L*-Asn-*L*-Val-OH (**6c**)

Yield: 91.7%; mp: 155.0–158.0 °C; ¹H NMR (CD₃OD, 300 Hz): δ 7.28–7.17 (m, 3H), 7.04–6.96 (m, 2H), 6.92–6.89 (m, 3H), 6.77 (d, 1H, *J* = 8.1 Hz), 4.71 (t, 1H, *J* = 6.6 Hz), 4.21 (d, 1H, *J* = 4.5 Hz), 3.46 (s, 2H), 2.69–2.62 (m, 1H), 2.57–2.49 (m, 1H), 2.10–1.99 (m, 1H), 0.79 (t, 6H, *J* = 6.6 Hz); ¹³C NMR (DMSO-*d*₆, 125 Hz): δ 173.2, 171.9, 171.5, 170.5, 157.1, 156.9, 138.7, 130.5, 130.2, 124.7, 123.8, 119.9, 119.0, 117.0, 57.5, 49.9, 42.2, 37.2, 30.4, 19.5, 18.0; MS-ESI *m/z*: 442 [M+H]⁺.

6.2.4. *N*-2-(3-phenoxyphenyl)acetyl-*L*-Asn-*L*-Val-*L*-allo-Thr-OBn (**6d**)

Yield: 84.7%; mp: 180.0–183.0 °C ¹H NMR (CD₃OD, 300 Hz): δ 7.29–7.17 (m, 8H), 7.05–6.96 (m, 2H), 6.92–6.89 (m, 3H), 6.77 (d, 1H, *J* = 8.7 Hz), 5.14–5.05 (m, 2H), 4.67 (t, 1H, *J* = 6.6 Hz), 4.36 (d, 1H, *J* = 6.0 Hz), 4.16 (d, 1H, *J* = 6.0 Hz), 4.00–3.93 (m, 1H), 3.47 (s, 2H), 2.70–2.63 (m, 1H), 2.56–2.49 (m, 1H), 2.04–1.98 (m, 1H), 1.17–1.13 (m, 3H), 0.78–0.72 (m, 6H); ¹H NMR (DMSO-*d*₆, 400 Hz): δ 8.40 (d, 1H, *J* = 8.0 Hz), 8.26 (d, 1H, *J* = 8.0 Hz), 7.54 (d, 1H,

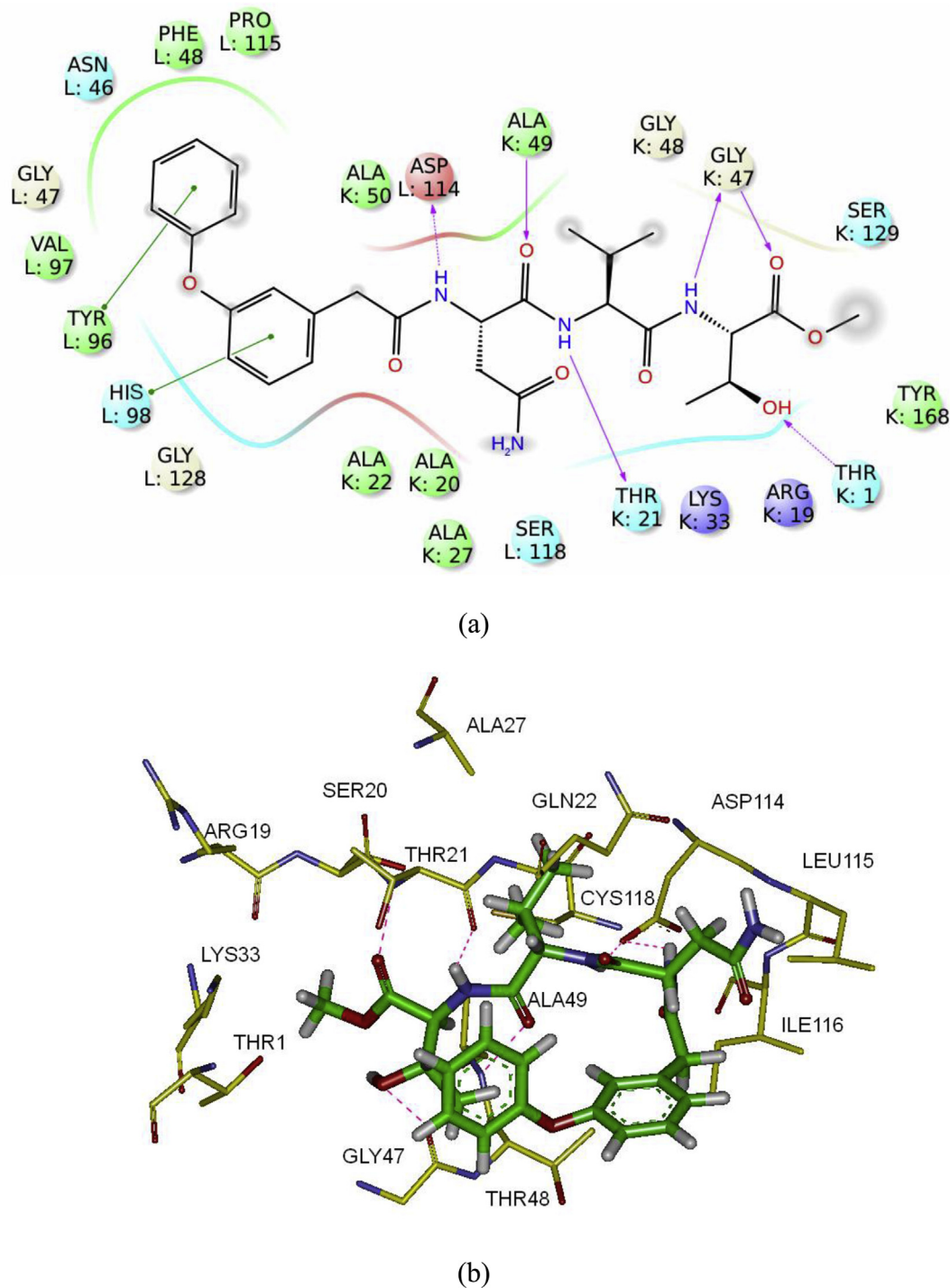


Fig. 5. The interaction mode of compound **6e** proposed by docking study. (a) 2D-plots: Residues marked with the letter "K" represents amino acids from the $\beta 5$ subunit of the 20S proteasome, while those with the letter "L" are from the $\beta 6$ subunit. (b) 3D-plots: The red dotted lines represents hydrogen bonding interactions. (For interpretation of the references to color in this figure caption, the reader is referred to the web version of this article.)

$J = 8.0$ Hz), 7.40–7.31 (m, 8H), 7.28 (t, 1H, $J = 8.0$ Hz), 7.13 (t, 1H, $J = 8.0$ Hz), 7.04–6.99 (3H), 6.94 (s, 1H), 6.89–6.83 (m, 2H), 5.10 (s, 2H), 5.05 (t, 1H, $J = 4.0$ Hz), 4.60 (d, 1H, $J = 8.0$ Hz), 4.25 (m, 2H), 3.93 (m, 1H), 3.46 (s, 2H), 2.55 (dd, 1H, $J = 16.0, 16.0$ Hz), 2.35 (dd, 1H, $J = 8.0, 16.0$ Hz), 1.90 (m, 1H), 1.10 (d, 3H, $J = 8.0$ Hz), 0.73 (d, 3H, $J = 8.0$ Hz), 0.65 (d, 3H, $J = 8.0$ Hz); ^{13}C NMR (DMSO- d_6 , 125 Hz): δ 172.0, 171.4, 171.2, 170.8, 170.4, 157.1, 156.9, 138.7, 136.4, 130.5, 130.1, 128.8, 128.4, 128.2, 124.7, 123.8, 119.9, 119.0, 117.0, 66.8, 66.2, 59.2, 57.2, 50.1, 42.2, 37.2, 31.3, 20.3, 19.5, 17.8; MS-ESI m/z : 633

$[\text{M}+\text{H}]^+$.

6.2.5. *N*-2-(3-phenoxyphenyl)acetyl-L-Asn-L-Val-L-allo-Thr-OMe (**6e**)

Yield: 64.6%; mp: 203.0–206.0 °C; ^1H NMR (CD $_3$ OD, 300 Hz): δ 7.27 (t, 2H, $J = 6.0$ Hz), 7.21 (t, 1H, $J = 6.0$ Hz), 7.05–6.98 (m, 2H), 6.92–6.90 (m, 3H), 6.78 (d, 1H, $J = 6.0$ Hz), 4.68 (t, 1H, $J = 5.1$ Hz), 4.31 (d, 1H, $J = 4.2$ Hz), 4.17 (d, 1H, $J = 4.8$ Hz), 4.01–3.95 (m, 1H), 3.64 (s, 3H), 3.47 (s, 2H), 2.72–2.66 (m, 1H), 2.58–2.52 (m, 1H),

2.08–1.99 (m, 1H), 1.16 (d, 3H, $J = 4.8$ Hz), 0.83–0.78 (m, 6H); ^{13}C NMR (DMSO- d_6 , 125 Hz): δ 172.0, 171.4, 171.2, 170.4, 157.1, 156.9, 138.7, 130.5, 130.1, 124.7, 123.8, 119.9, 119.0, 117.0, 66.8, 59.1, 57.3, 52.0, 50.1, 42.2, 37.2, 31.2, 20.4, 19.4, 17.9; MS-ESI m/z : 557 $[\text{M}+\text{H}]^+$.

6.2.6. *N*-2-(3-phenoxyphenyl)acetyl-L-Asn-L-Val-L-allo-Thr-OH (**6f**)

Yield: 99.0%; mp: 215.0–218.0 °C; ^1H NMR (CD $_3$ OD, 300 Hz): δ 7.27 (t, 2H, $J = 5.7$ Hz), 7.20 (t, 1H, $J = 6.0$ Hz), 7.04–6.98 (m, 2H), 6.92–6.90 (m, 3H), 6.77 (d, 1H, $J = 6.0$ Hz), 4.69 (t, 1H, $J = 4.8$ Hz), 4.33 (d, 1H, $J = 3.9$ Hz), 4.19 (d, 1H, $J = 4.5$ Hz), 4.05–3.99 (m, 1H), 3.47 (s, 2H), 2.71–2.66 (m, 1H), 2.58–2.52 (m, 1H), 2.09–2.00 (m, 1H), 1.17 (d, 3H, $J = 4.8$ Hz), 0.84–0.79 (m, 6H); ^{13}C NMR (DMSO- d_6 , 125 Hz): δ 172.3, 172.0, 171.2, 171.1, 170.4, 157.1, 156.9, 138.7, 130.5, 130.2, 124.7, 123.8, 119.9, 119.0, 117.0, 66.0, 58.9, 57.3, 50.1, 42.2, 37.2, 31.3, 20.1, 19.5, 17.9; HRMS-ESI m/z : 543.2440 $[\text{M}+\text{H}]^+$, calcd for C $_{27}\text{H}_{35}\text{O}_8\text{N}_4$: 543.2449.

6.2.7. *N*-2-(3-phenoxyphenyl)acetyl-L-Asn-L-Val-OBz (**6g**)

Yield: 36.0%; mp: 123.0–127.0 °C; ^1H NMR (CD $_3$ OD, 300 Hz): δ 7.29–7.16 (m, 8H), 7.04–6.96 (m, 2H), 6.91–6.88 (m, 3H), 6.76 (dt, 1H, $J = 8.1, 1.5$ Hz), 5.13–5.01 (m, 2H), 4.72 (t, 1H, $J = 6.6$ Hz), 4.26 (d, 1H, $J = 4.8$ Hz), 3.45 (s, 2H), 2.65–2.58 (m, 1H), 2.55–2.47 (m, 1H), 2.08–1.97 (m, 1H), 0.78–0.72 (m, 6H); ^{13}C NMR (DMSO- d_6 , 125 Hz): δ 171.9, 171.8, 171.6, 170.4, 157.1, 156.9, 138.7, 136.3, 130.5, 130.1, 128.9, 128.6, 128.5, 124.7, 123.8, 119.9, 119.0, 117.0, 66.4, 57.8, 49.8, 42.2, 37.4, 30.4, 19.3, 18.3; MS-ESI m/z : 532 $[\text{M}+\text{H}]^+$.

6.2.8. *N*-2-(3-phenoxyphenyl)acetyl-L-Asn-L-Val-NH(CH $_2$) $_2$ Ph (**6h**)

Yield: 83.7%; mp: 243.0–245.0 °C; ^1H NMR (DMSO- d_6 , 300 Hz): δ 8.40 (d, 1H, $J = 7.8$ Hz), 8.02 (t, 1H, $J = 5.4$ Hz), 7.61 (d, 1H, $J = 8.7$ Hz), 7.41–7.36 (m, 3H), 7.31–7.25 (m, 3H), 7.20–7.10 (m, 4H), 7.05–6.95 (m, 5H), 6.86–6.82 (m, 1H), 4.66–4.59 (m, 1H), 4.05 (t, 1H, $J = 7.8$ Hz), 3.46 (s, 2H), 3.33–3.20 (m, 2H), 2.69 (t, 2H, $J = 7.8$ Hz), 2.61–2.54 (m, 1H), 2.42–2.35 (m, 1H), 1.96–1.87 (m, 1H), 0.73–0.65 (m, 6H); ^{13}C NMR (DMSO- d_6 , 125 Hz): δ 172.1, 171.3, 170.9, 170.4, 157.1, 156.9, 139.8, 138.8, 130.5, 130.1, 129.1, 128.8, 126.5, 124.7, 123.8, 119.9, 119.0, 117.0, 58.0, 50.1, 42.2, 40.6, 37.3, 35.5, 30.7, 19.6, 17.8; MS-ESI m/z : 545 $[\text{M}+\text{H}]^+$.

6.2.9. *N*-2-(3-phenoxyphenyl)acetyl-L-Asn-L-Val-(R)-NHCH(CH $_3$)Ph (**6i**)

Yield: 88.1%; mp: 261.0–263.0 °C; ^1H NMR (DMSO- d_6 , 300 Hz): δ 8.38 (d, 1H, $J = 8.1$ Hz), 8.26 (d, 1H, $J = 8.1$ Hz), 7.69 (d, 1H, $J = 9.0$ Hz), 7.40–7.35 (m, 3H), 7.30–7.19 (m, 5H), 7.03–6.89 (m, 5H), 6.82 (d, 1H, $J = 7.5$ Hz), 4.91 (t, 1H, $J = 7.2$ Hz), 4.65–4.58 (m, 1H), 4.13–4.08 (m, 1H), 4.05–3.98 (m, 1H), 3.44 (s, 2H), 2.58–2.53 (m, 1H), 2.40–2.33 (m, 1H), 2.01–1.94 (m, 1H), 1.31 (d, 3H, $J = 7.2$ Hz), 0.76 (d, 3H, $J = 6.9$ Hz), 0.70 (d, 3H, $J = 6.6$ Hz); ^{13}C NMR (DMSO- d_6 , 125 Hz): δ 172.0, 171.4, 170.3, 170.1, 157.1, 156.9, 144.9, 138.8, 130.5, 130.1, 128.7, 127.1, 126.5, 124.7, 123.8, 119.9, 119.0, 117.0, 58.1, 50.1, 48.3, 42.2, 37.3, 30.8, 22.9, 19.6, 18.0; MS-ESI m/z : 545 $[\text{M}+\text{H}]^+$.

6.2.10. *N*-2-(3-phenoxyphenyl)acetyl-L-Asn-L-Val-(S)-NHCH(CH $_3$)Ph (**6j**)

Yield: 30.6%; mp: 243.0–246.0 °C; ^1H NMR (CD $_3$ OD, 300 Hz): δ 7.30–7.13 (m, 8H), 7.06–6.98 (m, 2H), 6.93–6.91 (m, 3H), 6.78 (d, 1H, $J = 7.8$ Hz), 4.91 (q, 1H, $J = 6.9$ Hz), 4.71 (t, 1H, $J = 6.6$ Hz), 4.11 (d, 1H, $J = 5.7$ Hz), 3.48 (s, 2H), 2.75–2.68 (m, 1H), 2.60–2.52 (m, 1H), 2.06–1.99 (m, 1H), 1.39 (d, 3H, $J = 7.2$ Hz), 0.74 (d, 6H, $J = 6.9$ Hz); ^{13}C NMR (DMSO- d_6 , 150 Hz): δ 172.0, 171.3, 170.4, 170.1, 157.1, 156.9, 145.2, 138.7, 130.5, 130.1, 128.6, 127.0, 126.4, 124.7, 123.8, 119.9, 119.0, 117.0, 57.8, 50.2, 48.4, 42.2, 37.3, 31.0, 23.0, 19.6, 17.8; MS-ESI m/z : 545 $[\text{M}+\text{H}]^+$.

6.2.11. *N*-2-(3-phenoxyphenyl)acetyl-L-Asn-L-Val-NH-(2-hydroxy-4-methoxybenzyl) (**6k**)

Yield: 31.5%; mp: 201.0–203.0 °C; ^1H NMR (CD $_3$ OD, 300 Hz): δ 7.29–7.17 (m, 3H), 7.05–6.96 (m, 3H), 6.92–6.89 (m, 3H), 6.77 (d, 1H, $J = 8.7$ Hz), 6.29–6.27 (m, 2H), 4.68 (t, 1H, $J = 6.9$ Hz), 4.18 (s, 2H), 4.12–4.06 (m, 1H), 3.64 (s, 3H), 3.46 (s, 2H), 2.72–2.64 (m, 1H), 2.57–2.50 (m, 1H), 2.07–1.98 (m, 1H), 0.75 (t, 6H, $J = 4.8$ Hz); ^{13}C NMR (DMSO- d_6 , 125 Hz): δ 172.1, 171.6, 171.4, 170.3, 159.8, 157.1, 156.9, 156.2, 138.8, 130.5, 130.1, 129.8, 124.7, 123.8, 119.9, 119.0, 117.9, 117.0, 104.6, 101.6, 57.9, 55.4, 50.1, 42.2, 37.6, 37.3, 30.8, 19.6, 17.9; MS-ESI m/z : 577 $[\text{M}+\text{H}]^+$.

6.2.12. *N*-2-(3-phenoxyphenyl)acetyl-L-Asn-L-Val-NH-(2,4-dimethoxybenzyl) (**6l**)

Yield: 81.3%; mp: 217.0–222.0 °C; ^1H NMR (DMSO- d_6 , 300 Hz): δ 8.47 (d, 1H, $J = 7.5$ Hz), 8.199 (m, 1H), 7.67 (d, 1H, $J = 9.3$ Hz), 7.43 (s, 1H), 7.37 (t, 2H, $J = 7.5$ Hz), 7.27 (t, 1H, $J = 7.8$ Hz), 7.11 (t, 1H, $J = 7.2$ Hz), 7.04–6.94 (m, 5H), 6.88 (s, 1H), 6.83 (d, 1H, $J = 7.2$ Hz), 6.51 (d, 1H, $J = 2.1$ Hz), 6.43 (d, 1H, $J = 8.1$ Hz), 4.62–4.59 (m, 1H), 4.17–4.12 (m, 3H), 3.75 (s, 3H), 3.72 (s, 3H), 3.45 (s, 2H), 2.59–2.49 (m, 1H), 2.41–2.34 (m, 1H), 1.99–1.92 (m, 1H), 0.74–0.69 (m, 6H); ^{13}C NMR (DMSO- d_6 , 125 Hz): δ 172.1, 171.3, 171.0, 170.4, 160.0, 158.0, 157.1, 156.9, 138.8, 130.5, 130.1, 129.0, 124.7, 123.8, 119.9, 119.3, 119.0, 117.0, 104.6, 98.5, 58.1, 55.8, 55.6, 50.3, 42.2, 37.3, 30.8, 19.6, 17.9; MS-ESI m/z : 591 $[\text{M}+\text{H}]^+$.

6.2.13. *N*-2-(3-phenoxyphenyl)acetyl-L-Gln-L-Val-NH-(2-hydroxy-4-methoxybenzyl) (**6m**)

yield: 75.6%; mp: 195.0–196.0 °C; ^1H NMR (DMSO- d_6 , 300 Hz): δ 8.29 (d, 2H, $J = 6.0$ Hz), 7.78 (d, 1H, $J = 6.0$ Hz), 7.36–7.24 (m, 4H), 7.11 (t, 1H, $J = 7.5$ Hz), 7.02–6.93 (m, 5H), 6.83–6.75 (m, 2H), 6.34–6.27 (m, 2H), 4.30–4.24 (m, 1H), 4.15–4.10 (m, 3H), 3.63 (s, 3H), 3.44 (s, 2H), 2.07–2.02 (m, 2H), 1.91–1.84 (m, 2H), 1.74–1.66 (m, 1H), 0.75–0.72 (m, 6H); ^{13}C NMR (DMSO- d_6 , 125 Hz): δ 174.3, 171.7, 170.4, 159.8, 157.1, 156.9, 139.0, 130.5, 130.1, 129.8, 124.7, 123.8, 119.8, 119.1, 117.8, 117.0, 101.7, 58.1, 55.3, 52.7, 42.3, 37.7, 32.1, 31.1, 28.4, 19.6, 18.4; HRMS-ESI m/z : 591.2800 $[\text{M}+\text{H}]^+$, calcd for C $_{26}\text{H}_{35}\text{N}_4\text{O}_7$: 591.2819.

6.2.14. *N*-2-(3-phenoxyphenyl)acetyl-L-Lys(Cbz)-L-Val-NH-(2-hydroxy-4-methoxybenzyl) (**6n**)

Yield: 62.2%; mp: 142.0–143.0 °C; ^1H NMR (DMSO- d_6 , 300 Hz): δ 9.55 (s, 1H), 8.27–8.20 (m, 2H), 7.74 (d, 1H, $J = 9.0$ Hz), 7.39–7.21 (m, 8H), 7.19–7.09 (m, 2H), 7.03–6.92 (m, 4H), 6.82 (d, 1H, $J = 7.8$ Hz), 6.36–6.28 (m, 2H), 4.99 (s, 2H), 4.27–4.22 (m, 1H), 4.18–4.04 (m, 3H), 3.64 (s, 3H), 3.44 (d, 2H, $J = 3.3$ Hz), 2.93–2.88 (m, 2H), 1.93–1.86 (m, 1H), 1.58–1.18 (m, 6H), 0.76–0.74 (m, 6H); ^{13}C NMR (DMSO- d_6 , 125 Hz): δ 172.0, 171.7, 170.3, 159.8, 157.1, 156.9, 156.5, 156.3, 139.1, 137.7, 130.5, 130.1, 129.9, 128.8, 128.2, 124.6, 123.8, 119.7, 119.0, 117.8, 117.0, 104.5, 101.6, 65.6, 58.1, 55.3, 53.0, 42.3, 40.7, 37.6, 32.0, 31.0, 29.6, 23.1, 19.6, 18.5; MS-ESI m/z : 724 $[\text{M}+\text{H}]^+$.

6.2.15. *N*-2-(3-phenoxyphenyl)acetyl-L-Lys-L-Val-NH-(2-hydroxy-4-methoxybenzyl) (**6o**)

Yield: 90.1%. mp: 165.0–166.0 °C; ^1H NMR (CD $_3$ OD, 300 Hz): δ 7.35–7.24 (m, 3H), 7.10–7.02 (m, 3H), 6.97–6.96 (m, 3H), 6.84 (d, 1H, $J = 8.0$ Hz), 6.32–6.35 (m, 2H), 4.33 (t, 1H, $J = 4.0$ Hz), 4.25 (d, 2H, $J = 8.0$ Hz), 4.10 (d, 1H, $J = 8.0$ Hz), 3.71 (s, 3H), 3.52 (s, 2H), 2.59 (t, 2H, $J = 4.0$ Hz), 2.05–1.95 (m, 1H), 1.78–1.42 (m, 6H), 0.87–0.84 (m, 6H); ^{13}C NMR (DMSO- d_6 , 125 Hz): δ 172.1, 170.9, 170.2, 161.1, 157.1, 157.0, 156.9, 139.2, 130.5, 130.1, 130.0, 124.7, 123.8, 119.7, 119.0, 118.0, 117.0, 104.2, 101.7, 58.2, 55.3, 53.0, 42.3, 42.2, 37.8, 32.5, 30.9, 30.4, 23.1, 19.6, 18.5; MS-ESI m/z : 591 $[\text{M}+\text{H}]^+$.

6.3. Proteasome assay

The 20S proteasome activity was determined using a Calbiochem proteasome assay kit following the manufacturer's protocol. The chymotrypsin-like activity of the proteasome was assayed by incubating the proteasome (0.5 µg/ml) with the fluorogenic substrate Suc-LLVY-AMC (20 µM) in the presence of proteasome activators and tested compounds. The trypsin-like and caspase-like activities of the 20S proteasome were determined using the fluorogenic substrates Bz-VGR-AMC and (Z)-LLE-bNA, respectively. Cleavage of the substrates by the proteasome resulted in emission of fluorescence, which was measured and expressed as the rate of the reaction by using a Biotek fluorometer. The rate of the cleavage reaction is defined as dF/dt, where dF/dt is the change of fluorescence intensity over time. IC₅₀, calculated by using CalcuSin, is the compound concentration that resulted in 50% decrease in the reaction rate.

6.4. Molecular modeling

The structure of compound **6e** was generated and molecular docking was performed with the Discovery Studio 2.5 software package (Accelrys, San Diego, USA). The structure of the 20S proteasome (β5 and β6 subunits) was obtained from the Protein Data Bank (PDB code: 3SDK). The docking calculation was carried out with the Ligandfit protocol. Default settings were used. All calculations were performed on a DELL Precision T5500 workstation. Maestro (version 9.3, Schrödinger, LLC, New York) was used to plot the 2D interaction modes.

Acknowledgment

Support for this research was provided by the 863 Hi-Tech Program (2012AA020302) and the National Natural Science Foundation of China (81302703).

Appendix A. Supplementary data

Supplementary data related to this article can be found at <http://dx.doi.org/10.1016/j.ejmech.2015.05.023>.

References

- [1] L. Bedford, J. Lowe, L.R. Dick, R.J. Mayer, J.E. Brownell, *Nat. Rev. Drug Disc.* 10 (2011) 29–46.
- [2] L. Borissenko, M. Groll, *Chem. Rev.* 107 (2007) 687–717.
- [3] R. Bold, *Cancer Invest* 22 (2004) 328–329.
- [4] K. Redic, *J. Pharm. Pharmacol.* 65 (2013) 1095–1106.
- [5] N. Micale, K. Scarbaci, V. Troiano, R. Ettari, S. Grasso, M. Zappalà, *Med. Res. Rev.* 34 (2014) 1001–1069.
- [6] V. Troiano, K. Scarbaci, R. Ettari, N. Micale, C. Cerchia, A. Pinto, T. Schirmeister, E. Novellino, S. Grasso, A. Lavecchia, M. Zappalà, *Eur. J. Med. Chem.* 83 (2014) 1–14.
- [7] A. Bordessa, M. Keita, X. Maréchal, L. Formicola, N. Lagarde, J. Rodrigo, G. Bernadat, C. Bauvais, J.-L. Soulier, L. Dufau, T. Milcent, B. Crousse, M. Reboud-Ravaux, S. Onger, *Eur. J. Med. Chem.* 70 (2013) 505–524.
- [8] M. Hasegawa, Y. Yasuda, M. Tanaka, K. Nakata, E. Umeda, Y. Wang, C. Watanabe, S. Uetake, T. Kunoh, M. Shionyu, R. Sasaki, I. Shiina, T. Mizukami, *Eur. J. Med. Chem.* 71 (2014) 290–305.
- [9] L. Piovan, P. Milani, M.S. Silva, P.G. Moraes, M. Demasi, L.H. Andrade, *Eur. J. Med. Chem.* 73 (2014) 280–285.
- [10] K. Scarbaci, V. Troiano, N. Micale, R. Ettari, L. Tamborini, C.D. Giovanni, C. Cerchia, S. Grasso, E. Novellino, T. Schirmeister, A. Lavecchia, M. Zappalà, *Eur. J. Med. Chem.* 76 (2014) 1–9.
- [11] J. Kohno, Y. Koguchi, M. Nishio, K. Nakao, M. Kuroda, R. Shimizu, T. Ohnuki, S. Komatsubara, *J. Org. Chem.* 65 (2000) 990–995.
- [12] Y. Koguchi, J. Kohno, M. Nishio, K. Takahashi, T. Okuda, T. Ohnuki, S. Komatsubara, *J. Antibiot.* 53 (2000) 105–109.
- [13] M. Groll, Y. Koguchi, R. Huber, J. Kohno, *J. Mol. Biol.* 311 (2001) 543–548.
- [14] Z.-Q. Yang, B.H.B. Kwok, S. Lin, M.A. Koldobskiy, C.M. Crews, S.J. Danishefsky, *Chem. Bio. Chem.* 4 (2003) 508–513.
- [15] M. Kaiser, M. Groll, C. Siciliano, I. Assfalg-Machleidt, E. Weyher, J. Kohno, A.G. Milbradt, C. Renner, R. Huber, L. Moroder, *Chem. Bio. Chem.* 5 (2004) 1256–1266.
- [16] M. Kaiser, A. Milbradt, C. Siciliano, I. Assfalg-Machleidt, W. Machleidt, M. Groll, C. Renner, L. Moroder, *Chem. Biodiv.* 1 (2004) 161–173.
- [17] M. Groll, M. Gotz, M. Kaiser, E. Weyher, L. Moroder, *Chem. Biol.* 13 (2006) 607–614.
- [18] N. Basse, S. Piguel, D. Papapostolou, A. Ferrier-Berthelot, N. Richey, M. Pagano, P. Sarthou, J. Sobczak-Thépot, M. Reboud-Ravaux, J. Vidal, *J. Med. Chem.* 50 (2007) 2842–2850.
- [19] M. Groll, N. Gallastegui, X. Maréchal, V. Le Ravalec, N. Basse, N. Richey, E. Genin, R. Huber, L. Moroder, J. Vidal, M. Reboud-Ravaux, *Chem. Med. Chem.* 5 (2010) 1701–1705.
- [20] D.R. Micklem, P. Ruurs, C. Sylvain, Y. Lu, K.D. Shenk, M.K. Bennett, F. Parlati, S.J. Lee, M. Aujay, E. Suzuki, K. Levitsky, J.B. Lorens, *Blood* 114 (2009) 3439–3447.
- [21] R.T. Lum, S.S. Kerwar, S.M. Meyer, M.G. Nelson, S.R. Schow, D. Shiffman, M.M. Wick, A. Joly, *Biochem. Pharmacol.* 55 (1998) 1391–1397.
- [22] R.T. Lum, M.G. Nelson, A. Joly, A.G. Horsma, G. Lee, S.M. Meyer, M.M. Wick, S.R. Schow, *Bioorg. Med. Chem. Lett.* 8 (1998) 209–214.
- [23] C. Blackburn, K.M. Gigstad, P. Hales, K. Garcia, M. Jones, F.J. Bruzzese, C. Barrett, J.X. Liu, T.A. Soucy, D.S. Sappal, N. Bump, E.J. Olhava, P. Fleming, L.R. Dick, C. Tsu, M.D. Sintchak, J.L. Blank, *Biochem. J.* 430 (2010) 461–476.
- [24] C. Blackburn, C. Barrett, J.L. Blank, F.J. Bruzzese, N. Bump, L.R. Dick, P. Fleming, K. Garcia, P. Hales, Z. Hu, M. Jones, J.X. Liu, D.S. Sappal, M.D. Sintchak, C. Tsu, K.M. Gigstad, *Bioorg. Med. Chem. Lett.* 20 (2010) 6581–6586.
- [25] C. García-Echeverría, P. Imbach, D. France, P. Fürst, M. Lang, M. Noorani, D. Scholz, J. Zimmermann, P. Furet, *Bioorg. Med. Chem. Lett.* 11 (2001) 1317–1319.
- [26] P. Furet, P. Imbach, P. Fürst, M. Lang, M. Noorani, J. Zimmermann, C. García-Echeverría, *Bioorg. Med. Chem. Lett.* 11 (2001) 1321–1324.
- [27] P. Furet, P. Imbach, P. Fuerst, M. Lang, M. Noorani, J. Zimmermann, C. García-Echeverría, *Bioorg. Med. Chem. Lett.* 12 (2002) 1331–1334.
- [28] P. Furet, P. Imbach, M. Noorani, J. Koeppler, K. Laumen, M. Lang, V. Guagnano, P. Fuerst, J. Roesel, J. Zimmermann, C. García-Echeverría, *J. Med. Chem.* 47 (2004) 4810–4813.
- [29] L. Huang, D. Yu, P. Ho, K. Qian, K.-H. Lee, C.-H. Chen, *Bioorg. Med. Chem.* 16 (2008) 6696–6701.